



# Limitations of 2-pool models in representing different time-scale dynamics of particulate and mineral-associated organic carbon

Franco Fernandez-Catinot<sup>1,2,†</sup>, Wanjia Hu<sup>1,3,†</sup>, Agustin Sarquis<sup>4,5</sup>, María Victoria Vaieretti<sup>2,6</sup>, Natalia Perez-Harguindeguy<sup>2,6</sup>, Xiaojuan Feng<sup>3</sup>, Carlos A. Sierra<sup>1</sup>

5 <sup>1</sup>Max Planck Institute for Biogeochemistry, Jena, 07745, Germany

<sup>2</sup>Instituto Multidisciplinario de Biología Vegetal (UNC-CONICET) Córdoba, 5016, Argentina

<sup>3</sup>State Key Laboratory of Forage Breeding-by-Design and Utilization, and Key Laboratory of Vegetation and Environmental Change, Institute of Botany, Chinese Academy of Sciences, Beijing, 100093, China

10 <sup>4</sup>Instituto de Investigaciones Fisiológicas y Ecológicas Vinculadas a la Agricultura, (UBA-CONICET), Buenos Aires, Argentina

<sup>5</sup>Cátedra de Ecología, Facultad de Agronomía, Universidad de Buenos Aires, Buenos Aires, Argentina

15 <sup>6</sup>Departamento de Diversidad Biológica y Ecología, Facultad de Ciencias Exactas, Físicas y Naturales, Universidad Nacional de Córdoba, Argentina

#Equally contributed to this work

*Correspondence to:* Franco Fernandez-Catinot ([ffernandez@bgc-jena.mpg.de](mailto:ffernandez@bgc-jena.mpg.de) or [ffernandezcatinot@imbiv.unc.edu.ar](mailto:ffernandezcatinot@imbiv.unc.edu.ar))

**Abstract.** In the last decade, the conceptual framework that characterizes soil organic carbon (SOC) into particulate organic carbon (POC) and mineral-associated organic carbon (MAOC) fractions has gained traction in studies of C dynamics. This SOC characterization is useful for developing empirical studies and for parsimonious model parameterizations. However,

20 rigorous testing of model structures incorporating the POC-MAOC framework is still lacking, in particular tests involving simultaneous measurements of C pool changes and respiration fluxes. We conducted an incubation experiment using control and litter-addition treatments, measuring changes in SOC fraction contents and respiration fluxes throughout the incubation.

Then, we applied an inverse modelling approach to compare the performance of 2-pool (POC-MAOC) and 3-pool models (which also included a faster-cycling litter C pool) to reproduce the observed data. We then calculated the C ages and transit

25 times to explore the predicted C persistence. Finally, we performed simulations to evaluate the effects of different model structures and parameterizations on SOC persistence. For both treatments, we observed that 2-pool models were unable to simultaneously reproduce the changes in C pool contents and respiration, while the 3-pool models adequately predicted both variables and yielded lower C ages and transit times. The fact that 3-pool models outperformed 2-pool models even for control soils, indicates that POC represents a heterogeneous pool that should be modelled as distinct compartments. We discuss that

30 2-pool models collapse POC dynamics operating at different timescales into a single one, failing to capture the different respiration phases and the gradual C pool changes. In contrast, 3-pool models distributed C processes operating at different timescales among compartments: the litter C pool captured faster-cycling dynamics, allowing POC and MAOC to better represent intermediate- and long-term dynamics, respectively. We also found that both model structure and changes in key



parameters affected C persistence estimations. Models that included shorter pathways to MAOC, or allowed faster transfers  
35 into more persistent pools, predicted higher C age and transit time. This study highlights the limitations of representing SOC  
dynamics exclusively through POC and MAOC and shows how model structure shapes SOC contents and persistence  
estimates. Rather than advocating a specific model configuration, our results suggest that SOC models should explicitly  
40 represent processes operating across multiple timescales, which, depending on the ecosystem context, may require  
incorporating additional C compartments beyond the POC-MAOC framework. Furthermore, as transfer rates play a key role  
in determining SOC persistence, it is important to better understand and quantify how C is transferred toward MAOC and how  
these processes can be represented in models.

## 1 Introduction

Soil organic carbon (SOC) represents the largest terrestrial active carbon (C) pool, accruing globally more than 2.000 Pg C in  
the first meter (Jobbágy and Jackson, 2000). SOC plays a crucial role in addressing some of the major humanity's challenges,  
45 including climate change, soil quality, and water and food security (IPCC, 2022; Lal, 2016; Smith et al., 2015). As SOC  
contents have declined over thousands of years of human land use (Sanderman et al., 2017), it is critical to preserve and even  
increase SOC stocks worldwide. In this context, terrestrial biogeochemical models represent important tools for predicting  
changes in terrestrial SOC and its responses to global change drivers, as they enhance our understanding of C stabilization and  
decomposition (Campbell and Paustian, 2015; Shi et al., 2018; Wieder et al., 2018).  
50 In the last decade, there has been an increased interest in the separation of SOC into mineral-associated organic carbon  
(MAOC) and particulate organic carbon (POC). As these fractions are formed by different mechanisms and controlled by  
different factors, their distinction can improve our understanding of overall SOC dynamics (Cotrufo et al., 2013; Lavallee et  
al., 2019; Stewart et al., 2008). On the one hand, MAOC is formed by organo-mineral bonds between organic C, mainly  
produced by microbial re-synthesis, and the soil's fine mineral particles. These associations represent a strong chemical  
55 protection against mineralization, providing MAOC with relatively high persistence (Kögel-Knabner et al., 2008; Sokol and  
Bradford, 2019; Von Lützow et al., 2007). On the other hand, POC is predominantly formed by light-weight plant-derived  
fragments at various stages of decomposition. The C in this fraction does not establish organo-mineral bonds; instead, POC  
protection relies on aggregate occlusion and on its biochemical recalcitrance against mineralization, having a lower persistence  
60 (Von Lützow et al., 2007). Hence, the biochemical traits of different plant materials might be important in determining the  
short- and medium-term decomposition dynamics of POC, despite the fact that all organic structures can be eventually broken  
down and mineralized (Lehmann and Kleber, 2015; Marschner et al., 2008).

As SOC represents a heterogeneous C pool, incorporating the POC and MAOC pools into soil biogeochemical models can  
enhance our understanding of SOC dynamics and its drivers (Campbell and Paustian, 2015; Robertson et al., 2019; Zhang et  
al., 2021). This minimal SOC characterization is convenient for developing empirical studies and for parameterizing  
65 parsimonious models to predict SOC contents and persistence. Indeed, recent studies applying 2-pool models based on POC



and MAOC have already proved useful for analyzing SOC processes (e.g., Campbell and Paustian, 2015; Georgiou et al., 2024; Guo et al., 2022; Sokol et al., 2022; Zhou et al., 2024). However, 2-pool models restricted to POC and MAOC may not always adequately capture SOC dynamics. This is because POC is typically modelled as a homogeneous pool, even though, like bulk SOC, it can contain both labile and recalcitrant compounds (Cotrufo and Lavallee, 2022; Schrumpf et al., 2013).

70 Therefore, 2-pool models assume that POC operates on a single time-scale, despite its components might cycle over both shorter and longer temporal scales. Although the POC-MAOC models have become increasingly popular in SOC modelling, rigorous testing of model structures is still lacking, particularly tests involving simultaneous changes in different C pool contents and respiration fluxes. For this reason, it is essential to evaluate how accurately these models capture SOC dynamics (Garsia et al., 2023; Le Noë et al., 2023).

75 Furthermore, alternative model structures might lead to different predictions (Shi et al., 2018; Wieder et al., 2018). Such differences can arise from alternative theoretical approaches about C formation pathways, which reflect distinct C transfers among pools (Tao et al., 2024). One modelling approach is to assume that Litter C first enters the POC pool and, through subsequent decomposition and re-synthesis, is transferred into the MAOC pool (e.g., Guo et al., 2022; Zhou et al., 2024).

80 Alternatively, Litter C may enter directly into both the POC and MAOC pools, rather than assuming that MAOC forms exclusively through POC transformation (Cotrufo and Lavallee, 2022). These different C formation pathways might affect the predicted C persistence in each pool and within the overall system. Moreover, changes in key parameter values, particularly when combined with different model structures, may also lead to contrasting predictions of C persistence (Tao et al., 2024).

85 SOC dynamics can be modelled using compartmental dynamical systems: models characterized by homogeneous compartments that evolve over time according to parameters that describe their decomposition and the transfers among them (Sierra et al., 2012; Sierra and Müller, 2015). Depending on the number of theoretical compartment and the connections assumed in the model, the pathways that C atoms take as they travel through the soils system may be very different (Metzler and Sierra, 2025). The transit time (i.e., how long it takes for C atoms since they enter the system until they leave) is a useful metric for analyzing the tortuosity of C pathways and C persistence in different systems. In addition, the age of C atoms stored in the soil can also be a useful metric, as it represents the time elapsed since the C entered the system until the time of

90 observation (Manzoni et al., 2009; Sierra et al., 2017). The estimation of these system-level metrics, transit time and C age, can be very informative for comparing the effects of different model structures on C persistence and overall persistence.

In this study we explored how different model structures based on the POC-MAOC paradigm affected the estimations of C pool contents and C persistence. We conducted a laboratory incubation experiment which evaluated two types of systems: 1) control soils without litter additions, and 2) soils with litter-additions. Throughout the incubation we quantified soil respiration rates; and at the beginning, middle and at the end of the incubation we measured soil's POC and MAOC contents. This design allowed us to systematically assess the performance of 2-pool models when fitted to the observed data, comparing their estimations with those of 3-pool models. In addition, we performed simulations using 2- and 3-pool models with different structures and parameter changes, aiming to evaluate how these differences affect the predicted C age and transit time of the system. Through the combination of experimental manipulations and modelling, we addressed the following questions: 1) Are



100 POC-MAOC 2-pool models sufficient to accurately predict SOC dynamics, in particular when estimating C contents and respiration rates simultaneously? 2) Among 2 and 3-pool models, which one performs best at predicting both C contents and respiration rates? and 3) Do different model structures and parameterizations produce similar C persistence estimates?

## 2 Materials and Methods

### 2.1 Study area, soil sampling, incubation experiments and analysis

105 We sampled soils from a high plateau located in the upper belt of the Cordoba mountain grasslands in central Argentina (2100 m above sea level, 31°34' S, 64°50' W). In this region, the mean temperatures of the coldest and warmest months are 5.1 and 11.5 °C, respectively, with no frost-free period. The mean annual precipitation is 900 mm, with most rainfall concentrated in the warmest months, between October and April. Soils are mostly Mollisols (Lithic Hapludolls), derived from weathering of granitic substrates and fine-textured eolian deposits (Cabido et al., 1987). The soil clays are dominated by biotite and illite, 110 with a smaller proportion of kaolinite (Pasquini et al., 2002). The soil pH is 5.0 on average (Vaieretti et al., 2013).

We sampled soils from short grasslands, a vegetation community dominated by short annual and perennial grasses and forbs (e.g., *Muhlenbergia peruviana* (P. Beauv.) Steud. and *Lachemilla pinnata* (Ruiz & Pav.; Vaieretti et al., 2018, 2013). For this, we collected four compound soil samples (eight subsamples) from the 0–5 cm depth (4 replicates). Once collected, we sieved the soils through a 2 mm mesh, and we determined their soil water content using the gravimetric method.

115 For the incubation experiments, we placed 50 g of soil in 125 ml flasks. We applied two treatments: 1) control soils with no-litter addition, and 2) soils with litter-additions of 1 g of *M. peruviana*. The added litter was cut in small fragments (<2 mm) and mixed in the soil matrix. We selected *M. peruviana* because it is a dominant species in short grasslands, and also because of its high decomposability, in comparison to other grass species from the region (Poca et al., 2014; Vaieretti et al., 2013, 2018). We employed two time-sets of samples, as we destructively harvested them after 3 and 6 months of incubation (16 120 samples in total = 2 treatments x 2 incubation times x 4 replicates). This design also allowed us to have 8 replicates for respiration measurements until month 3, and 4 replicates until month 6. Throughout the incubation we maintained the soils at 25°C and at field capacity (47% water content; Cassel and Nielsen, 1986). To measure the soil respiration, we built closed microcosms where we placed the soils along a flask with water to avoid desiccation, placed CO<sub>2</sub> traps using a flask with NaOH 1 M, and quantified the trapped CO<sub>2</sub> by titration. We measured the accumulated respiration at 7, 15, 28, 42, 63, 91, 136 and 125 182 days after the beginning of the incubation.

We measured the MAOC and POC contents of the soils before and after the incubations. For this we used the Duval et al., (2018) and Pestoni et al., (2020) techniques for MAOC and POC fractionation. Briefly, 10 g of air-dried soil <2 mm was dispersed in 100 mL of distilled water and ten glass beads (5 mm diameter) were added to increase aggregate destruction. The samples were subjected to mechanical dispersion through a rotary shaker (200 rpm) for 24 h. The soil suspension was poured 130 through a 53 µm pore sieve using a water flow to separate the POC and MAOC fractions. These materials were washed into a



dry dish, oven dried at 80°C, and weighed. Then, we determined the MAOC, POC, and total C contents using the Walkley and Black technique (Nelson and Sommers, 1996).

### 2.2.1 Models applied to data

In order to evaluate the performance of 2- and 3-pool models applied to the results of our experimental incubations, we used 135 an inverse modelling optimization (*i.e.*, procedure that estimates unknown parameters based on empirical observations). These models are commonly used in ecology and agriculture to estimate parameters that describe, for example, unknown pool sizes like C pool contents using mass loss data (Sarquis and Sierra, 2023). In this work, we applied these models to assess their performance by comparing their estimations to the observed C pool contents and respiration data. For this, we used the SoilR (Sierra et al., 2012) and the FME (Soetaert and Petzoldt, 2010) packages in R (R Core Team, 2024).

140 First, we built 2 and 3-pool models with connection in series, which can be expressed in matrix form as Eq. (1) (Sierra et al., 2012):

$$\frac{dC}{dt} = I + A \cdot C, \quad \text{with } C(t_0) = C_0 \quad (1)$$

where  $C$  is a  $m \times 1$  vector of C contents in  $m$  pools;  $A$  is a  $m \times m$  square matrix containing the decomposition rates for each pool and the transfer coefficients between pools; and  $I$  is a column vector describing the amount of C inputs to each pool  $m$ .

145 In our particular case,  $I = 0$  because there are not inputs during the incubation and the litter-addition treatment only occurs once at the beginning of the incubation, so it can be treated as an initial condition ( $C_0$ ). This initial condition can be included in different pools depending on the model assumptions, as explained below.

We built a 2-pool model consisting of 1) *Litter C + POC* pool, and 2) *MAOC* pool. For control soils, *Litter C*=0. For litter-addition treatments, we can combine the Litter C and POC and use a 2-pool approach. This is because the added litter consists 150 in senescent plant material smaller than 2 mm mixed within the soil matrix, in accordance with the particulate organic carbon concept (Lavallee et al., 2019). These 2-pool models can be expressed as Eq. (2):

$$\frac{dC}{dt} = \begin{bmatrix} -k_1 & 0 \\ a_{2,1} & -k_2 \end{bmatrix} \begin{bmatrix} \text{Litter C + POC} \\ \text{MAOC} \end{bmatrix}, \quad (2)$$

where the entries in the diagonal represent the decomposition rate  $k$  for each compartment  $j$ , and  $a_{ij}$  is the transfer coefficient from pool  $j$  to pool  $i$ . This means that the *Litter C + POC* and *MAOC* pools decompose at a  $k_1$  and  $k_2$  rate, respectively, and 155 that a fraction of the decomposed *Litter C + POC* forms new *MAOC* at a rate given by  $a_{2,1}$ .

Second, we applied a 3-pool model consisting of 1) *Litter C* pool, 2) *POC* pool and 3) *MAOC* pool. For litter-addition treatments, this option assumes that the added litter C is, in fact, different from POC and needs to be modelled separately. This is because although the added litter falls within the POC size range, it consists of fresh, more labile plant material that cycles faster, justifying to model it as a distinct compartment. As the control soils did not include litter, to apply this 3-pool model 160 we assumed an arbitrary value of 10% of the POC to function as an additional pool, which again we can name as “Litter C”. These models can be expressed as Eq. (3):



$$\frac{dc}{dt} = \begin{bmatrix} -k_1 & 0 & 0 \\ a_{2,1} & -k_2 & 0 \\ a_{3,1} & a_{3,2} & -k_3 \end{bmatrix} \begin{bmatrix} LitterC \\ POC \\ MAOC \end{bmatrix}, \quad (3)$$

In this model, the *Litter C*, *POC* and *MAOC* pools decompose at a  $k_1$ ,  $k_2$  and  $k_3$  rate, respectively, and a fraction of the decomposed *Litter C* forms new *POC* at a rate  $a_{2,1}$  and new *MAOC* at a rate  $a_{3,1}$ , while a fraction of the decomposed *POC* forms new *MAOC* at a rate  $a_{3,2}$ .

We applied the models described in Eq. 2 and Eq. 3 using the observed C contents in each C pool at the beginning, middle and at the end of the incubation, as well as the C respiration measured throughout the experiment. We plotted the model estimations alongside with the observed data. To evaluate the performance of the models, a common approach is to examine the Akaike Information Criterion (AIC, *i.e.*, metric that accounts for both goodness of fit and model complexity) and the Mean Squared Error (MSE, *i.e.*, the mean of the squared differences between predicted and observed values), selecting the model with the lowest values of both.

Before fitting the models, we ran a collinearity test following the procedure by Soetaert and Petzoldt (2010). This is a test that determines if the parameters are functionally related, meaning that changes in a parameter can be compensated by changes in others. If the test results in a high collinearity index ( $>20$ ), it indicates that different parameter sets can have similar probabilities, and thus it is not possible to determine a unique parameter set for a model (Sierra et al., 2015). In contrast, a low collinearity index ( $<20$ ) indicates that a unique parameter set for a model can be found, and, therefore, the model is suited for data assimilation. From this test we found that all the proposed models had a low collinearity index (Supplementary Fig. 1). It is worth noting that when applying an inverse modelling approach, the combined use of respiration data together with C pool contents substantially constrains parameter estimations and helps reduce collinearity.

## 180 2.2.2 C age and transit time estimations

We calculated the probability density functions of C age and transit time predicted by the 2-pool and 3-pool models applied to the control soils and litter-addition treatments. The probability density function describes the distribution of transit times or C ages of C atoms within a system. Using transit time as an example, a probability density function concentrated at low transit times indicates that most of the C leaves the system quickly, whereas a smaller fraction leaves it more slowly. The probability density function of C age for models of the form of equation (1) at steady state can be computed as follows (Eq. (4); Metzler and Sierra, 2018):

$$f(a) = -1^T \cdot A \cdot e^{a \cdot A} \cdot \frac{c}{\sum c} \quad (4)$$

where  $a$  is the random variable C age,  $1^T$  is the transpose of the m-dimensional vector containing ones,  $e^{a \cdot A}$  is the matrix exponential computed for each value of  $a$ , and  $\sum c$  is the sum of the stocks of all pools at steady state. The mean value of the probability densities function of C age can be computed by the following expression (Eq. (5)):



$$E(a) = -1^T \cdot A^{-1} \cdot \frac{c}{\sum c} \quad (5)$$

Similarly, the probability density function of transit time ( $\tau$ ) for these models is given by Metzler and Sierra, 2018 (Eq. (6)):

$$f(\tau) = -1^T \cdot A \cdot e^{\tau \cdot A} \cdot \frac{u}{\sum u}, \tau \geq 0 \quad (6)$$

and the mean transit time as Eq. (7)

195  $E(\tau) = -1^T \cdot A^{-1} \cdot \frac{u}{\sum u} \quad (7)$

### 2.3 Effects of model structure and parameter changes on estimated C persistence

Both differences in model structures and in parameters values might lead to different estimates of C persistence. To assess these effects, we examined how C persistence responds to 1) different model structures, 2) parameter changes, and 3) the combination of different model structures and parameter changes. For this, we ran simulations using the following 2- and a 3-pool models as a baseline, hereafter referred to as “2-Base” and “3-Base”, respectively (Fig. 1).

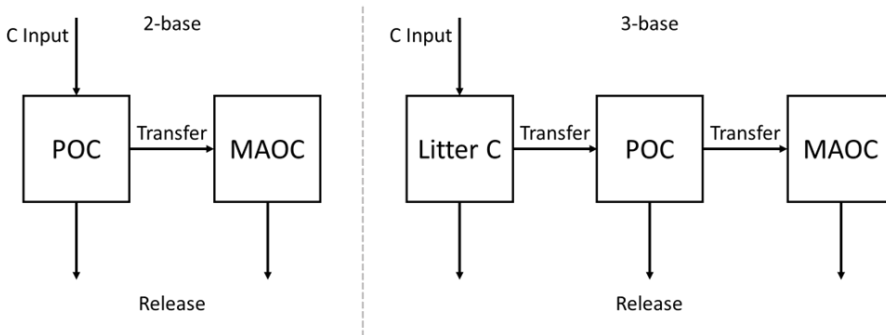


**Figure 1.** 2-Base and 3-Base models. The arrows represent the respiration fluxes (downwards arrows) and transfers processes (rightwards arrows) and not the full mathematical expressions.

In the 2-Base model, new C enters the system directly into the POC pool and is subsequently transferred to the MAOC pool, 205 as described in Eq. (8):

$$\frac{dc}{dt} = \begin{bmatrix} I(t) \\ 0 \end{bmatrix} + \begin{bmatrix} -k_1 & 0 \\ a_{2,1} & -k_2 \end{bmatrix} \begin{bmatrix} POC \\ MAOC \end{bmatrix}, \quad (8)$$

Where  $I(t)$  represents the C inputs in each time unit. In the 3-Base model, new C enters into the *Litter C* pool, is subsequently transferred to the POC pool, and finally to the MAOC pool, as described in Eq. (9):

$$\frac{dc}{dt} = \begin{bmatrix} I \\ 0 \\ 0 \end{bmatrix} + \begin{bmatrix} -k_1 & 0 & 0 \\ a_{2,1} & -k_2 & 0 \\ 0 & a_{3,2} & -k_3 \end{bmatrix} \begin{bmatrix} LitterC \\ POC \\ MAOC \end{bmatrix}, \quad (9)$$

210 To run the simulations, all the models received the same C input of 100 units per unit time. We applied the parameter values obtained from the optimization of the 3-pool models fitted to the litter-addition incubation treatments (Table 2) across all



model structures to ensure comparability. For the different model structures, we plotted the predicted probability density functions of C age and transit time and calculated their mean values. We used the following alternative model structures, shown in Table 1:

215

**Table 1.** Different model structures used for the model simulations

Model	Base structure	Description
<b>2-Base</b>	2-pool-model	Baseline model
<b>2.A</b>	2-pool-model	10% of C inputs enter directly into MAOC.
<b>3-Base</b>	3-pool-model	Baseline model
<b>3.A</b>	3-pool-model	Adds a direct C transfer from Litter C to MAOC ( $a_{31}$ ).
<b>3.B</b>	3-pool-model	Triples the decomposition rate of Litter C ( $k_1$ ).
<b>3.C</b>	3-pool-model	Triples $k_1$ and the transfer rate from Litter C to POC ( $a_{21}$ ).
<b>3.D</b>	3-pool-model	Triples $k_1$ , $a_{21}$ and the transfer rate from POC to MAOC ( $a_{32}$ ).
<b>3.E</b>	3-pool-model	Extends model 3.A by additionally tripling $k_1$ , $a_{21}$ and $a_{32}$ .
<b>3.F</b>	3-pool-model	Extends model 3.E by additionally tripling $a_{31}$ .

### 3 Results

#### 3.1 3-pool models performed better for both control and litter-addition treatments

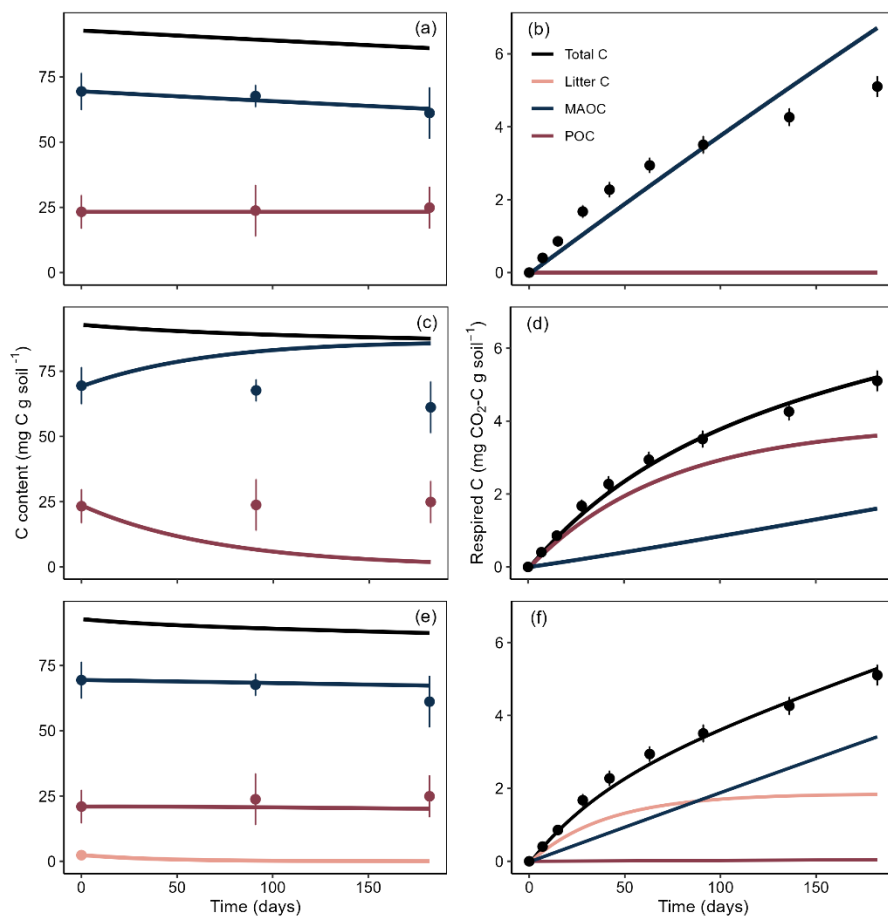
##### 3.1.1 Control soils

220 When we applied the 2-pool model to the control soils, we found two different sets of parameters that fitted the observed data (Table 2). The first set of parameters predicted well the observed C contents in each pool (POC and MAOC), but produced poor predictions for the respiration data (Fig. 2a, b; Table 2). In particular, this model showed the highest AIC and MSE values (Table 3). In contrast, the second set of parameters predicted the respiration data well, but had poor predictions for the C contents in each pool (Fig. 2c, d; Table 2). In this case, this model had intermediate AIC and MSE values (Table 3). When we 225 applied the 3-pool model we found a single set of parameters that yielded good predictions for both the C contents and the respiration data (Fig. 2e, f; Table 2). This model presented the lowest AIC and MSE values overall (Table 3). These values



were 2.19 and 1.47 times lower for AIC and 17.56 and 4.63 times lower for MSE compared with the 2-pool models that fitted the C contents and respiration data, respectively.

These results show that, although the control soils were assumed to be composed only of POC and MAOC, the 2-pool model  
 230 could not accurately predict the C contents and respiration simultaneously. In contrast, the 3-pool model performed better, providing good predictions for both C pool contents and respiration. This suggests that POC in the control soils was indeed heterogeneous, as including a third pool (10% of POC as Litter C, which showed a faster cycling, Table 2), better captured its C dynamics.



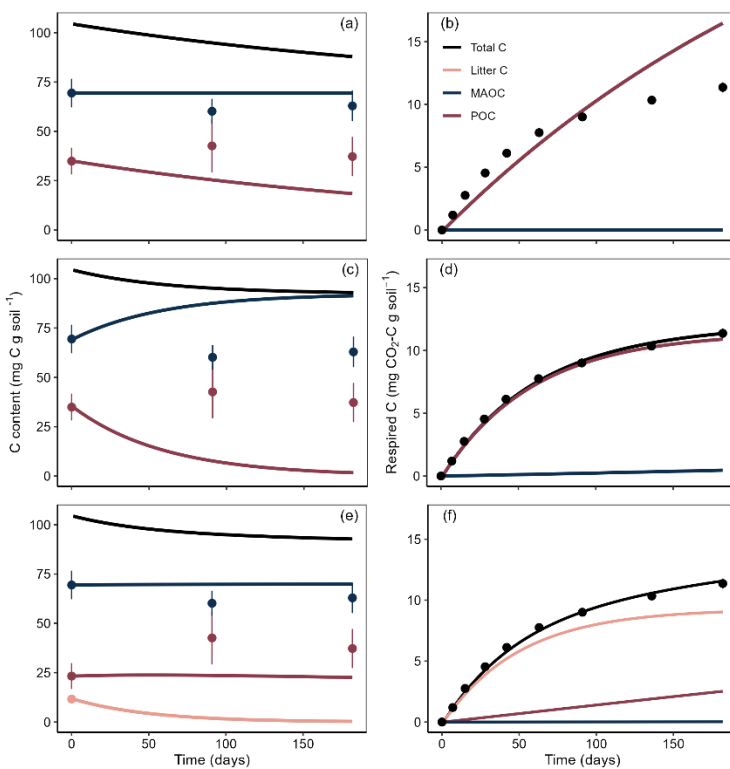
235

**Figure 2.** C content (left panels) and respiration (right panels) in each C pool and total in control soils (no litter-addition). In black, Total C; in dark blue, MAOC; in dark red, POC; in pink, Litter C. The lines represent the model estimations, while the points represent the observed data. (a) and (b): 2-pool models that best fitted C pools content. (c) and (d): 2-pool models that best fitted the respiration. (e) and (f): 3-pool model.



240 **3.1.2 Litter-addition treatments**

We found a similar pattern between the results from the control and from the litter-addition treatments. For the 2-pool model, we found two different sets of parameters that fitted the observed data (Table 2). The first set of parameters attempted to predict the observed C contents in each pool, although the model ended up underestimating the predicted POC contents and producing poor predictions for the respiration data (Fig. 3a, b; Table 2). This model had the highest AIC and MSE values (Table 3). The 245 second set of parameters fitted well the respiration data but produced poor predictions for the C contents (Fig. 3c, d; Table 2). This model had intermediate AIC and MSE values (Table 3). Finally, when we applied the 3-pool model, we found a single 250 set of parameters that yielded good predictions for both the respiration and C contents data (Fig. 3e, f; Table 2), although they were less accurate than those of the control soils (Fig. 2e, f). Consistent with the control soils results, the 3-pool model had the lowest AIC and MSE values (Table 3). These values were 1.85 and 1.12 times lower for AIC and 26.13 and 2.82 times lower for MSE compared with the 2-pool models that fitted the C contents and respiration data, respectively. The poor predictions resulting from the 2-pool models application highlight that, indeed, the added litter does not behave as POC, and it should be modelled as a separated C pool that cycles faster.



255 **Figure 3.** C content (left panels) and respiration C (right panels) in each C pool and total in litter-addition treatments. In black, Total C; in dark blue, MAOC; in dark red, POC; in pink, Litter C. The lines represent the model estimations, while the points represent the observed data. (a) and (b) 2-pool models that best fitted C pools content. (c) and (d) 2-pool models that best fitted the respiration. (e) and (f) 3-pool model.



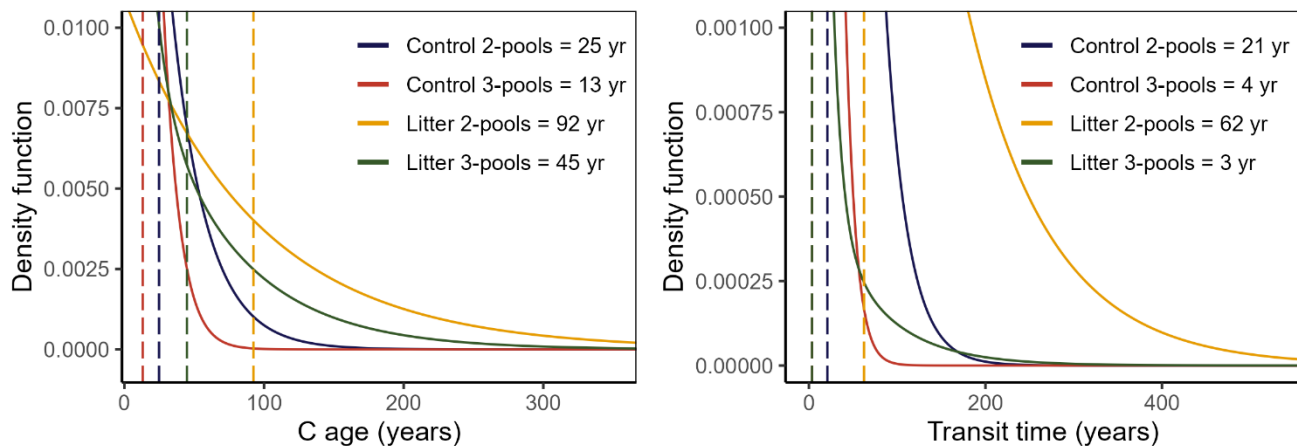
**Table 2. Parameter sets and relative content** of the initial ( $C_i$ ) and final ( $C_f$ ) C pools estimated for the 2- and 3-pool models applied to the incubation data. The “Data fitted” row indicates which variables were best fitted by each parameter set.

Data fitted	Control soils			Litter-addition treatment		
	2-pool model		3-pool model	2-pool model		3-pool model
	C contents	Respiration	Both variables	C contents	Respiration	Both variables
$k_1$	2.65E-05	5.074	9.195	1.279	6.124	6.856
$k_2$	0.204	0.040	0.121	8.09E-10	0.011	0.099
$k_3$	-	-	0.100	-	-	0.0162
$a_{21}$	0.014	0.832	0.173	1.01E-04	0.673	0.100
$a_{32}$	-	-	0.968	-	-	0.022
$a_{31}$	-	-	0.031	-	-	0.035
<b>Litter<sub>i</sub></b>	-	-	0.025	-	-	0.112
<b>Litter<sub>f</sub></b>	-	-	2.72E-04	-	-	0.004
<b>POC<sub>i</sub></b>	0.251	0.251	0.226	0.335	0.335	0.223
<b>POC<sub>f</sub></b>	0.271	0.021	0.230	0.210	0.018	0.250
<b>MAOC<sub>i</sub></b>	0.749	0.749	0.749	0.665	0.665	0.665
<b>MAOC<sub>f</sub></b>	0.729	0.979	0.769	0.790	0.982	0.746

Decomposition rates and transfer coefficients are expressed in  $\text{yr}^{-1}$

### 260 3.1.3 C age and transit time estimations in control and litter-addition treatments

For both control soils and litter-addition treatments, we observed that the 2-pool model that best fitted the respiration data estimated C age and transit time distributions with longer tails and higher mean values than the 3-pool models (Fig. 4). This indicates that the 2-pool model predicted higher C persistence, with C cycling more slowly and remaining in the system for longer periods. In contrast, the 3-pool models estimated faster C transit through the system, resulting in overall younger C 265 within the system. The probability density functions of C age and transit time from the 2-pool models that fitted the C content data (Table 2) are not shown, as they predicted unrealistic mean values, which exceeded tens of thousands of years. This was mainly driven by their predicted MAOC decomposition rates, which were extremely low.



270 **Figure 4.** Solid lines show the probability density distribution and dashed lines show the mean values of C age and transit time for the 2-pool model that best fitted respiration data and 3-pool models applied to control soils and litter-addition treatments. The 2-pool models that best fitted C contents are not shown, as their C ages and transit time estimations were the order of tens of thousands of years.

**Table 3.** AIC and MSE values for the 2- and 3-pool models applied to the incubation soils. The “Data fitted” column indicates which variables were best fitted by each parameter set.

Sample	Model	Data fitted	AIC	MSE
Control soils	2-pool	C pools	4.04	8.59
	2-pool	Respiration	2.71	2.27
	3-pool	Both variables	1.84	0.49
Litter-addition treatments	2-pool	C pools	5.65	42.88
	2-pool	Respiration	3.42	4.62
	3-pool	Both variables	3.08	1.69

### 3.2 Model comparison: effects of structures and parameters changes



### 3.2.1 Effects of model's structure changes on C stabilization

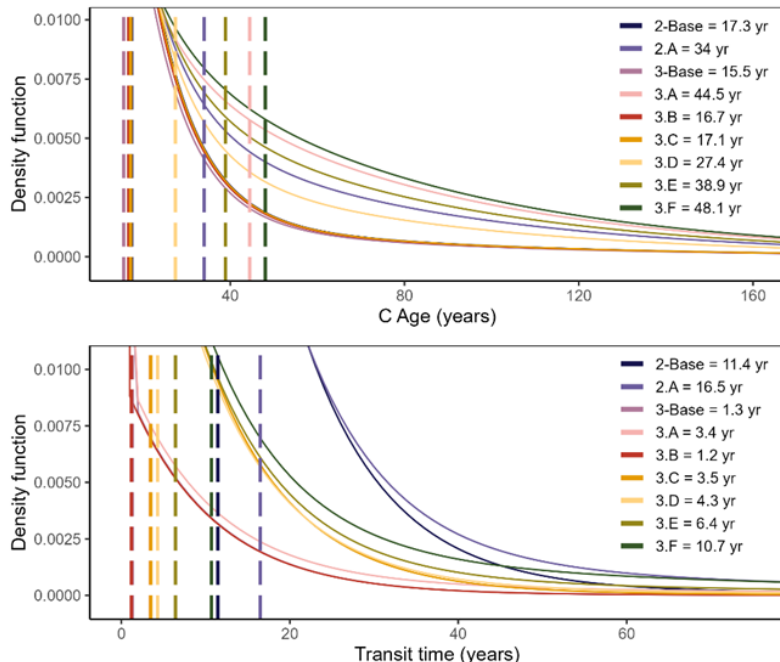
To evaluate the effects of model's structure changes on C stabilization, we compared the estimated mean C age and mean transit time across models that differed in how C is transferred among pools (Table 1). In the 2-pool model where 10% of C inputs enter MAOC directly (Model 2.A), both the mean C age and transit time increased compared to the 2-Base model (approximately 96% and 44% higher, respectively; Fig. 5). Likewise, in the 3-pool model where Litter C can transfer directly to MAOC (Model 3.A), the mean C age and transit time also increased compared to the 3-Base model (approximately 187% and 161% higher, respectively; Fig. 5). Overall, when the model structure allowed C to bypass the intermediate POC pool to the more persistent MAOC pool, the system retained C for longer periods, indicating a higher C persistence.

### 3.2.2 Effects of parameters changes on C stabilization

When we compared the estimated mean C age and mean transit time between the 3-Base model and the models in which the parameters were modified (Table 1), we observed that tripling the decomposition rate of the Litter C pool (Model 3.B) produced relatively small changes compared to the baseline (approximately a 7% increase in mean C age and a 7% decrease in mean transit time). When, in addition, the transfer rate from Litter C to POC was tripled (Model 3.C), the mean C age increased slightly (10%), but the mean transit time increased substantially (169%). When all three parameters were tripled (Model 3.D), including the transfer rate from POC to MAOC, the mean C age and mean transit time increased (approximately 77% and 230% higher, respectively). Overall, these results show that modifying the Litter C decomposition rate had little effects on C stabilization, but when the transfer rates increased, the rapid passage from more labile to more persistent pools markedly increased the system C persistence.

### 3.2.3 Effects of combined parameters and model structure changes on C stabilization

When we compared the estimated mean C age and mean transit time between the 3-Base model and models that combined structural and parameter changes (Table 1) we found that the model with a direct transfer pathway from Litter C to MAOC, together with tripled rates for Litter C decomposition and for transfers from Litter C to POC and from POC to MAOC (Model 3.E), substantially increased both mean C age and mean transit time compared to the baseline (approximately 151% and 392%, respectively). In the model that, in addition to these changes, also tripled the direct transfer rate from Litter C to MAOC (Model 3.F), the mean C age increased further, whereas mean transit time increased much more strongly (approximately 210% and 723%, respectively). These results indicate that both model structure and parameter changes have important effects on predicted C persistence. However, the responses of C age and mean transit time were not equal. The mean C age increased across models, reaching values up to 210%, whereas mean transit time showed a much stronger response, increasing consistently up to 723% in models with more complex structures that allowed Litter C to directly enter more persistent pools.



305

**Figure 5.** Solid lines show the probability density function and dashed lines show the mean values of C age and transit time for models with different structures and parameters.

#### 4 Discussion

##### 4.1 3-pool models performed better both for control and litter-addition treatments.

310 Over more than 80 years, and especially in recent decades, a wide variety of soil C models have been developed to describe and quantify SOC stocks and their persistence across a broad range of ecosystems and changing scenarios (Abramoff et al., 2018; Dangal et al., 2022; Manzoni and Porporato, 2009; Robertson et al., 2019; Zhang et al., 2021). While these models have proven to be highly useful in advancing our understanding of SOC dynamics (e.g., Georgiou et al., 2024; Gomes et al., 2019; Riggers et al., 2019; Zhang et al., 2024), their application still requires caution due to the implications of different model assumptions. In this study, we explored the performance of different model structures using both experimental and simulated data, aiming to assess whether the widely used 2- and 3-pool models are adequate for predicting SOC contents and their respiration dynamics.

315 Our findings indicate that 2-pool models were unable to capture both the C pool size changes and the respiration fluxes simultaneously. In contrast, 3-pool models were able to fit both response variables with a single set of parameters, yielding the lowest AIC and MSE values. It is important to highlight two key findings derived from the application of the models. First, it was almost self-evident that litter-addition treatments required a 3-pool structure, as fresh litter exhibit much faster



decomposition dynamics than POC and MAOC. However, this was not expected for control soils (no litter-addition), which were presumably composed only of POC and MAOC. The fact that even for control soils the 3-pool models outperformed the 325 2-pool models might be because POC represented, indeed, a heterogeneous pool that should be modelled as distinct compartments. As a result, 2-pool models collapsed POC dynamics operating at different timescales into a single one, failing to capture both the fast initial and the slower later respiration phases simultaneously with the gradual C pool changes throughout the incubation.

Second, the 3-pool models showed a markedly better capacity to capture both these faster and slower C dynamics for both 330 variables. This suggests that the underlying mechanism in the inclusion of a third pool, is enabling the model to distribute the processes operating at different time-scales into the different C compartments. Specifically, the Litter C pool captured the rapid-response respiration fluxes at the beginning of the incubation, showing decomposition rates on the order of months. This allowed the POC and MAOC pools to represent intermediate and slower C dynamics, with decomposition rates on the order of years and decades, respectively (Table 2). In the same line, both C ages and transit times were consistently lower for the 3- 335 pool models. This likely arises because these models estimate that the Litter C pool, which represents the C inputs to POC and MAOC, is rapidly respired and cycles quickly through the system. In contrast, in 2-pool models the respiration fluxes are driven by the longer timescale dynamics in the POC and MAOC pools, resulting in higher C persistence.

In recent decades, there has been a growing tendency to study SOC dynamics by conceptualizing SOC as POC and MAOC, 340 fractions that reflected faster and slower dynamics, respectively. By definition, POC consists primarily of light-weight compounds of plant origin at different stages of decomposition, whose composition can vary with plant community and soil depth (Cotrufo et al., 2013; Lavallee et al., 2019; Von Lützow et al., 2007; Wiesmeier et al., 2019). This reflects varying proportions of recently added material and older, more processed C. As such, POC may contain a mixture of organic matter 345 compounds with a wide range of decomposition and transfer rates. In this line, our results give empirical and conceptual evidence that POC consists of a heterogeneous pool with compounds that cycle at different rates. For our particular soils, these differences within POC were key drivers of the observed differences in the model's predictions and performance. In light of 350 our results, our goal is not to advocate for either 2- or 3-pool models, particularly given that several SOC models already employ a larger number of compartments (e.g., exchangeable and stable MAOC, free and occluded POC, dissolved organic C, microbial C; Abramoff et al., 2018; Manzoni et al., 2009; Witzgall et al., 2021; Zhang et al., 2021). Rather, our results emphasize that SOC models should explicitly represent processes operating across multiple temporal scales in ways that are appropriate for different systems and contexts, which may require combining experimental manipulations with modelling to evaluate model's performance. In our case, incorporating a third compartment beyond the POC-MAOC framework allowed us to reproduce the observed empirical dynamics, whereas in other contexts different model structures may be required.

#### 4.2 C persistence was primarily driven by direct transfers into more-persistent pools

When we simulated alternative models under different hypothetical scenarios and compared their estimates of C age and mean transit time to explore the effects of changes in parameters and model structure on C persistence, we observed that introducing



355 a direct pathway to the MAOC pool (either through direct C inputs or through transfers) increased both C age and transit time. This response likely reflects that bypassing the relatively unstable Litter C and POC pools reduces early C losses, allowing a larger fraction of C to be retained into the more persistent and slower-cycling MAOC pool (Cotrufo et al., 2015; Kleber et al., 2015; Zhou et al., 2024).

360 It is important to note that, when only parameter values were modified, the changes in the Litter C decomposition rate had little effect on predicted C persistence. In contrast, increasing transfer rates led to modest increases in C age but much stronger increases in transit time. This pattern suggests that transfer processes, rather than Litter C decomposition rate alone, play a dominant role in transit times by controlling how rapidly C moves from labile pools into more persistent pools. Notably, when the transfer rates were tripled (Model 3.C, 3.D), the predicted C persistence was similar or even higher to that obtained by adding a direct transfer pathway to MAOC (Fig. 5). This indicates that sufficiently high transfer rates can reproduce the effects 365 of explicitly adding a direct transfer pathway to MAOC, as both mechanisms result in rapid C transfer into the MAOC pool. When parameter and structural changes were combined, predicted C persistence increased substantially, particularly for transit time. In these scenarios, transit time values were approximately 7 times higher than those obtained for the baseline model, highlighting strong, non-additive interactions between model structure and key parameters (*i.e.*, transfer rates into the MAOC pool). Overall, these results indicate that transfers into the MAOC pool have a stronger influence on the predicted C persistence.

370 Therefore, when constructing models based on the POC-MAOC framework, assumptions regarding both model structure and transfer-related parameters should be carefully evaluated, as they can strongly influence estimates of C cycling and persistence. Model structure and transfer processes are particularly relevant in light of recent advances in our understanding of the factors that modulate transfers to the MAOC pool across ecosystems. For example, it is well established that MAOC formation efficiency is modulated by the saturation deficit, as well as by the presence of specific cations, such as oxalate-extractable Al 375 and Fe and exchangeable Ca (Barré et al., 2014; Beare et al., 2014; Castellano et al., 2015; Saidy et al., 2013; Six et al., 2002). Hence, soils rich in these cations or with low saturation deficits may exhibit higher effective transfer rates to MAOC, which could translate into higher transit times. Vegetation composition differences might also play an important role, as rhizodeposition has been shown to promote higher MAOC formation efficiency than root or aboveground inputs (Villarino et al., 2021; Yin et al., 2025). In addition, recent evidence suggests that existing MAOC can promote the formation of new 380 MAOC (King and Sokol, 2025), indicating potential feedbacks in transfer rates to MAOC. Despite these advances, further studies exploring MAOC formation are needed, as factors such as microbial carbon-use efficiency or C input rates have shown contradictory effects (King and Sokol, 2025; Sokol and Bradford, 2019; Wei et al., 2022; Yang et al., 2025).

385 Our results also suggest that transfer rates play a key role in determining SOC persistence. While current research has largely focused on quantifying SOC stocks and decomposition rates under different ecosystem contexts and management practices (*e.g.*, Deng et al., 2016; Georgiou et al., 2024, 2022; Zhou et al., 2024), less attention has been given to explicitly quantifying transfer rates between C compartments. Future research should aim to characterize how C is transferred and transformed towards MAOC, and how these processes are represented in models. Reducing uncertainties associated with transfer rates



among SOC compartments might be crucial for improving soil biogeochemical models and their ability to predict SOC persistence.

## 390 5 Conclusion

In our study, we found that 2-pool models including only POC and MAOC were not sufficient to simultaneously predict slow dynamics of SOC fractions changes and fast dynamics of respired CO<sub>2</sub> from incubations. Although 2-pool models captured one response variable well, they performed poorly when predicting C contents and respiration rates simultaneously. In contrast, 395 3-pool models performed adequately in predicting both variables at the same time. These performance differences likely arise from the limitations of 2-pool models in representing POC processes operating at different timescales, whereas the additional compartment in 3-pool models allows for a better representation of slow-, intermediate-, and fast-term dynamics. Due to the better representation of Litter C faster dynamics, the 3-pool models yielded lower transit times in comparison to 2-pool models 400 for both control and litter-addition treatments. Furthermore, both model structure and key parameter changes had important effects on the predicted C persistence. Models that included shorter pathways to MAOC, or that allowed faster transfers of C into more persistent pools, consistently produced higher estimates of C age and transit time. This highlights the importance of better understanding how C is transferred and transformed towards MAOC, and how these processes are represented in models. Overall, our study highlights the limitations of representing SOC dynamics exclusively through POC and MAOC pools, and 405 shows that model structure fundamentally shapes predictions of SOC fraction contents and persistence. Accordingly, SOC models should explicitly represent processes operating across multiple temporal scales, which may require different model structures depending on the ecosystem context. Future studies should therefore empirically test model performance by jointly evaluating the effects of C inputs on slow changes in C pool sizes and rapid respiration flux responses.

## Author contributions

FFC: Conceptualization, Writing – original draft preparation, Writing – review and editing, Investigation, Data curation, Formal analysis, Visualization, Methodology, Software, Funding acquisition, Project administration. WH: Conceptualization, 410 Writing – original draft preparation, Writing – review and editing, Data curation, Formal analysis, Methodology, Visualization. AS: Writing – review and editing, Methodology, Software. MVV: Writing – review and editing, Investigation, Conceptualization, Funding acquisition, Resources, Methodology. NPH: Writing – review and editing, Conceptualization, Investigation, Funding acquisition, Resources, Methodology. XF: Writing – review and editing. CS: Conceptualization, Writing – review and editing, Formal analysis, Supervision, Software.



#### 415 Competing interests

The authors declare that they have no known competing financial interests or personal relationships that could have appeared to influence the work reported in this paper.

#### Code and data availability

420 The data and the code used for modelling is available via a GitHub repository at <https://github.com/Holinwj/Model-POC-MAOC> (last access: February 7th, 2026).

#### Acknowledgements

We have used ChatGPT to improve the readability of some sentences at the end of the writing process.

#### 425 Financial support

The study was financially supported by the Consejo Nacional de Investigaciones Científicas y Técnicas (CONICET; PIP-112-201501-00387 CO); the Deutscher Akademischer Austauschdienst (DAAD; 57698958), and the China Scholarship Council (202404910492).

#### References

430 Abramoff, R., Xu, X., Hartman, M., O'Brien, S., Feng, W., Davidson, E., Finzi, A., Moorhead, D., Schimel, J., Torn, M., and Mayes, M. A.: The Millennial model: in search of measurable pools and transformations for modeling soil carbon in the new century, *Biogeochemistry*, 137, 51–71, <https://doi.org/10.1007/s10533-017-0409-7>, 2018.

Barré, P., Fernandez-Ugalde, O., Virto, I., Velde, B., and Chenu, C.: Impact of phyllosilicate mineralogy on organic carbon stabilization in soils: incomplete knowledge and exciting prospects, *Geoderma*, 235–236, 382–395, 435 <https://doi.org/10.1016/j.geoderma.2014.07.029>, 2014.

Beare, M. H., McNeill, S. J., Curtin, D., Parfitt, R. L., Jones, H. S., Dodd, M. B., and Sharp, J.: Estimating the organic carbon stabilisation capacity and saturation deficit of soils: a New Zealand case study, *Biogeochemistry*, 120, 71–87, <https://doi.org/10.1007/s10533-014-9982-1>, 2014.

Cabido, M., Breimer, R., and Vega, G.: Plant Communities and Associated Soil Types in a High Plateau of the Cordoba Mountains, Central Argentina, *Mt. Res. Dev.*, 7, 25, <https://doi.org/10.2307/3673322>, 1987.

Campbell, E. E. and Paustian, K.: Current developments in soil organic matter modeling and the expansion of model applications: a review, *Environ. Res. Lett.*, 10, 123004, <https://doi.org/10.1088/1748-9326/10/12/123004>, 2015.



Carvalho-Gomes, L., Faria, R. M., De Souza, E., Veloso, G. V., Schaefer, C. E. G. R., and Filho, E. I. F.: Modelling and mapping soil organic carbon stocks in Brazil, *Geoderma*, 340, 337–350, <https://doi.org/10.1016/j.geoderma.2019.01.007>, 445 2019.

Cassel, D. K. and Nielsen, D. R.: Field Capacity and Available Water Capacity, in: SSSA Book Series, vol. 5, edited by: Klute, A., Wiley, 901–926, <https://doi.org/10.2136/sssabookser5.1.2ed.c36>, 1986.

Castellano, M. J., Mueller, K. E., Olk, D. C., Sawyer, J. E., and Six, J.: Integrating plant litter quality, soil organic matter stabilization, and the carbon saturation concept, *Glob. Change Biol.*, 21, 3200–3209, <https://doi.org/10.1111/gcb.12982>, 2015.

450 Cotrufo, M. F. and Lalonde, J. M.: Soil organic matter formation, persistence, and functioning: A synthesis of current understanding to inform its conservation and regeneration, in: *Advances in Agronomy*, vol. 172, Elsevier, 1–66, <https://doi.org/10.1016/bs.agron.2021.11.002>, 2022.

Cotrufo, M. F., Wallenstein, M. D., Boot, C. M., Denef, K., and Paul, E.: The Microbial Efficiency-Matrix Stabilization (MEMS) framework integrates plant litter decomposition with soil organic matter stabilization: do labile plant inputs form 455 stable soil organic matter?, *Glob. Change Biol.*, 19, 988–995, <https://doi.org/10.1111/gcb.12113>, 2013.

Cotrufo, M. F., Soong, J. L., Horton, A. J., Campbell, E. E., Haddix, M. L., Wall, D. H., and Parton, W. J.: Formation of soil organic matter via biochemical and physical pathways of litter mass loss, *Nat. Geosci.*, 8, 776–779, <https://doi.org/10.1038/ngeo2520>, 2015.

460 Dangal, S. R. S., Schwalm, C., Cavigelli, M. A., Gollany, H. T., Jin, V. L., and Sanderman, J.: Improving Soil Carbon Estimates by Linking Conceptual Pools Against Measurable Carbon Fractions in the DAYCENT Model Version 4.5, *J. Adv. Model. Earth Syst.*, 14, e2021MS002622, <https://doi.org/10.1029/2021MS002622>, 2022.

Deng, L., Zhu, G., Tang, Z., and Shangguan, Z.: Global patterns of the effects of land-use changes on soil carbon stocks, *Glob. Ecol. Conserv.*, 5, 127–138, <https://doi.org/10.1016/j.gecco.2015.12.004>, 2016.

465 Duval, M. E., Galantini, J. A., Martínez, J. M., and Limbozzi, F.: Labile soil organic carbon for assessing soil quality: influence of management practices and edaphic conditions, *CATENA*, 171, 316–326, <https://doi.org/10.1016/j.catena.2018.07.023>, 2018.

Garsia, A., Moinet, A., Vazquez, C., Creamer, R. E., and Moinet, G. Y. K.: The challenge of selecting an appropriate soil organic carbon simulation model: A comprehensive global review and validation assessment, *Glob. Change Biol.*, 29, 5760–5774, <https://doi.org/10.1111/gcb.16896>, 2023.

470 Georgiou, K., Jackson, R. B., Vinodusková, O., Abramoff, R. Z., Ahlström, A., Feng, W., Harden, J. W., Pellegrini, A. F. A., Polley, H. W., Soong, J. L., Riley, W. J., and Torn, M. S.: Global stocks and capacity of mineral-associated soil organic carbon, *Nat. Commun.*, 13, 3797, <https://doi.org/10.1038/s41467-022-31540-9>, 2022.

Georgiou, K., Koven, C. D., Wieder, W. R., Hartman, M. D., Riley, W. J., Pett-Ridge, J., Bouskill, N. J., Abramoff, R. Z., Slessarev, E. W., Ahlström, A., Parton, W. J., Pellegrini, A. F. A., Pierson, D., Sulman, B. N., Zhu, Q., and Jackson, R. B.: 475 Emergent temperature sensitivity of soil organic carbon driven by mineral associations, *Nat. Geosci.*, 17, 205–212, <https://doi.org/10.1038/s41561-024-01384-7>, 2024.



Guo, X., Viscarra Rossel, R. A., Wang, G., Xiao, L., Wang, M., Zhang, S., and Luo, Z.: Particulate and mineral-associated organic carbon turnover revealed by modelling their long-term dynamics, *Soil Biol. Biochem.*, 173, 108780, <https://doi.org/10.1016/j.soilbio.2022.108780>, 2022.

480 IPCC (Ed.): *Climate change 2022: mitigation of climate change*, IPCC, Geneva, 1 pp., 2022.

Jobbágy, E. G. and Jackson, R. B.: THE VERTICAL DISTRIBUTION OF SOIL ORGANIC CARBON AND ITS RELATION TO CLIMATE AND VEGETATION, *Ecol. Appl.*, 10, 423–436, [https://doi.org/10.1890/1051-0761\(2000\)010%5B0423:TVDOSO%5D2.0.CO;2](https://doi.org/10.1890/1051-0761(2000)010%5B0423:TVDOSO%5D2.0.CO;2), 2000.

King, A. E. and Sokol, N. W.: Soil carbon formation is promoted by saturation deficit and existing mineral-associated carbon, not by microbial carbon-use efficiency, *Sci. Adv.*, 11, eadv9482, <https://doi.org/10.1126/sciadv.adv9482>, 2025.

485 Kleber, M., Eusterhues, K., Keilweit, M., Mikutta, C., Mikutta, R., and Nico, P. S.: Mineral–Organic Associations: Formation, Properties, and Relevance in Soil Environments, in: *Advances in Agronomy*, vol. 130, Elsevier, 1–140, <https://doi.org/10.1016/bs.agron.2014.10.005>, 2015.

Kögel-Knabner, I., Guggenberger, G., Kleber, M., Kandeler, E., Kalbitz, K., Scheu, S., Eusterhues, K., and Leinweber, P.: 490 Organo-mineral associations in temperate soils: Integrating biology, mineralogy, and organic matter chemistry, *J. Plant Nutr. Soil Sci.*, 171, 61–82, <https://doi.org/10.1002/jpln.200700048>, 2008.

Lal, R.: Soil health and carbon management, *Food Energy Secur.*, 5, 212–222, <https://doi.org/10.1002/fes3.96>, 2016.

Lavallee, J. M., Soong, J. L., and Cotrufo, M. F.: Conceptualizing soil organic matter into particulate and mineral-associated forms to address global change in the 21st century, *Glob. Change Biol.*, 26, 261–273, <https://doi.org/10.1111/gcb.14859>, 2019.

495 Le Noë, J., Manzoni, S., Abramoff, R., Bölscher, T., Bruni, E., Cardinael, R., Ciais, P., Chenu, C., Clivot, H., Derrien, D., Ferchaud, F., Garnier, P., Goll, D., Lashermes, G., Martin, M., Rasse, D., Rees, F., Sainte-Marie, J., Salmon, E., Schiedung, M., Schimel, J., Wieder, W., Abiven, S., Barré, P., Cécillon, L., and Guenet, B.: Soil organic carbon models need independent time-series validation for reliable prediction, *Commun. Earth Environ.*, 4, 158, <https://doi.org/10.1038/s43247-023-00830-5>, 2023.

500 Lehmann, J. and Kleber, M.: The contentious nature of soil organic matter, *Nature*, 528, 60–68, <https://doi.org/10.1038/nature16069>, 2015.

Manzoni, S. and Porporato, A.: Soil carbon and nitrogen mineralization: Theory and models across scales, *Soil Biol. Biochem.*, 41, 1355–1379, <https://doi.org/10.1016/j.soilbio.2009.02.031>, 2009.

Manzoni, S., Katul, G. G., and Porporato, A.: Analysis of soil carbon transit times and age distributions using network theories, 505 *J. Geophys. Res. Biogeosciences*, 114, 2009JG001070, <https://doi.org/10.1029/2009JG001070>, 2009.

Marschner, B., Brodowski, S., Dreves, A., Gleixner, G., Gude, A., Grootes, P. M., Hamer, U., Heim, A., Jandl, G., Ji, R., Kaiser, K., Kalbitz, K., Kramer, C., Leinweber, P., Rethemeyer, J., Schäffer, A., Schmidt, M. W. I., Schwark, L., and Wiesenberg, G. L. B.: How relevant is recalcitrance for the stabilization of organic matter in soils?, *J. Plant Nutr. Soil Sci.*, 171, 91–110, <https://doi.org/10.1002/jpln.200700049>, 2008.



510 Metzler, H. and Sierra, C. A.: Linear Autonomous Compartmental Models as Continuous-Time Markov Chains: Transit-Time and Age Distributions, *Math. Geosci.*, 50, 1–34, <https://doi.org/10.1007/s11004-017-9690-1>, 2018.

Metzler, H. and Sierra, C. A.: Information Content and Maximum Entropy of Compartmental Systems in Equilibrium, *Entropy*, 27, 1085, <https://doi.org/10.3390/e27101085>, 2025.

Nelson, D. W. and Sommers, L. E.: Total Carbon, Organic Carbon, and Organic Matter, in: *Methods of Soil Analysis. Part 3. Chemical Methods*, Madison, WI, 961–1010, 1996.

515 Pasquini, A. I., Lecomte, K. L., and Depetris, P. J.: Geoquímica de ríos de montaña en las Sierras Pampeanas: II. El río Los Reartes, sierra de Comenchingones, provincia de Córdoba, *Rev. Asoc. Geológica Argent.*, 59, 129–140, 2002.

Pestoni, S., Gallardo, N., Harguindeguy, N. P., and Kowaljow, E.: Influencia del método de dispersión en el fraccionamiento físico de un suelo de Argentina central, *Cienc. Suelo*, 38, 2020.

520 Poca, M., Pérez-Harguindeguy, N., Vaieretti, M. V., and Cingolani, A. M.: Descomposición y calidad físico-química foliar de 24 especies dominantes de los pastizales de altura de las sierras de Córdoba, Argentina, *Ecol. Austral*, 24, 249–257, <https://doi.org/10.25260/EA.14.24.2.0.28>, 2014.

R Core Team: R: A Language and Environment for Statistical Computing, 2024.

Riggers, C., Poeplau, C., Don, A., Bamminger, C., Höper, H., and Dechow, R.: Multi-model ensemble improved the prediction 525 of trends in soil organic carbon stocks in German croplands, *Geoderma*, 345, 17–30, <https://doi.org/10.1016/j.geoderma.2019.03.014>, 2019.

Robertson, A. D., Paustian, K., Ogle, S., Wallenstein, M. D., Lugato, E., and Cotrufo, M. F.: Unifying soil organic matter formation and persistence frameworks: the MEMS model, *Biogeosciences*, 16, 1225–1248, <https://doi.org/10.5194/bg-16-1225-2019>, 2019.

530 Saidy, A. R., Smernik, R. J., Baldock, J. A., Kaiser, K., and Sanderman, J.: The sorption of organic carbon onto differing clay minerals in the presence and absence of hydrous iron oxide, *Geoderma*, 209–210, 15–21, <https://doi.org/10.1016/j.geoderma.2013.05.026>, 2013.

Sanderman, J., Hengl, T., and Fiske, G. J.: Soil carbon debt of 12,000 years of human land use, *Proc. Natl. Acad. Sci.*, 114, 9575–9580, <https://doi.org/10.1073/pnas.1706103114>, 2017.

535 Sarquis, A. and Sierra, C. A.: Information content in time series of litter decomposition studies and the transit time of litter in arid lands, *Biogeosciences*, 20, 1759–1771, <https://doi.org/10.5194/bg-20-1759-2023>, 2023.

Schrumpf, M., Kaiser, K., Guggenberger, G., Persson, T., Kögel-Knabner, I., and Schulze, E.-D.: Storage and stability of organic carbon in soils as related to depth, occlusion within aggregates, and attachment to minerals, *Biogeosciences*, 10, 1675–1691, <https://doi.org/10.5194/bg-10-1675-2013>, 2013.

540 Shi, Z., Crowell, S., Luo, Y., and Moore, B.: Model structures amplify uncertainty in predicted soil carbon responses to climate change, *Nat. Commun.*, 9, 2171, <https://doi.org/10.1038/s41467-018-04526-9>, 2018.

Sierra, C. A. and Müller, M.: A general mathematical framework for representing soil organic matter dynamics, *Ecol. Monogr.*, 85, 505–524, <https://doi.org/10.1890/15-0361.1>, 2015.



Sierra, C. A., Müller, M., and Trumbore, S. E.: Models of soil organic matter decomposition: the SoilR package, version 1.0, 545 Geosci. Model Dev., 5, 1045–1060, <https://doi.org/10.5194/gmd-5-1045-2012>, 2012.

Sierra, C. A., Malghani, S., and Müller, M.: Model structure and parameter identification of soil organic matter models, Soil Biol. Biochem., 90, 197–203, <https://doi.org/10.1016/j.soilbio.2015.08.012>, 2015.

Sierra, C. A., Müller, M., Metzler, H., Manzoni, S., and Trumbore, S. E.: The muddle of ages, turnover, transit, and residence times in the carbon cycle, Glob. Change Biol., 23, 1763–1773, <https://doi.org/10.1111/gcb.13556>, 2017.

550 Six, J., Conant, R. T., Paul, E. A., and Paustian, K.: Stabilization mechanisms of soil organic matter: Implications for C-saturation of soils, Plant Soil, 241, 155–176, <https://doi.org/10.1023/A:1016125726789>, 2002.

Smith, P., Cotrufo, M. F., Rumpel, C., Paustian, K., Kuikman, P. J., Elliott, J. A., McDowell, R., Griffiths, R. I., Asakawa, S., Bustamante, M., House, J. I., Sobocká, J., Harper, R., Pan, G., West, P. C., Gerber, J. S., Clark, J. M., Adhya, T., Scholes, R. J., and Scholes, M. C.: Biogeochemical cycles and biodiversity as key drivers of ecosystem services provided by soils, SOIL, 555 1, 665–685, <https://doi.org/10.5194/soil-1-665-2015>, 2015.

Soetaert, K. and Petzoldt, T.: Inverse Modelling, Sensitivity and Monte Carlo Analysis in R Using Package **FME**, J. Stat. Softw., 33, <https://doi.org/10.18637/jss.v033.i03>, 2010.

Sokol, N. W. and Bradford, M. A.: Microbial formation of stable soil carbon is more efficient from belowground than aboveground input, Nat. Geosci., 12, 46–53, <https://doi.org/10.1038/s41561-018-0258-6>, 2019.

560 Sokol, N. W., Whalen, E. D., Jilling, A., Kallenbach, C., Pett-Ridge, J., and Georgiou, K.: Global distribution, formation and fate of mineral-associated soil organic matter under a changing climate: A trait-based perspective, Funct. Ecol., 36, 1411–1429, <https://doi.org/10.1111/1365-2435.14040>, 2022.

Stewart, C. E., Plante, A. F., Paustian, K., Conant, R. T., and Six, J.: Soil Carbon Saturation: Linking Concept and Measurable Carbon Pools, Soil Sci. Soc. Am. J., 72, 379–392, <https://doi.org/10.2136/sssaj2007.0104>, 2008.

565 Tao, F., Houlton, B. Z., Huang, Y., Wang, Y., Manzoni, S., Ahrens, B., Mishra, U., Jiang, L., Huang, X., and Luo, Y.: Convergence in simulating global soil organic carbon by structurally different models after data assimilation, Glob. Change Biol., 30, e17297, <https://doi.org/10.1111/gcb.17297>, 2024.

Vaieretti, M. V., Cingolani, A. M., Pérez Harguindeguy, N., and Cabido, M.: Effects of differential grazing on decomposition rate and nitrogen availability in a productive mountain grassland, Plant Soil, 371, 675–691, <https://doi.org/10.1007/s11104-013-1831-9>, 2013.

Vaieretti, M. V., Iamamoto, S., Pérez Harguindeguy, N., and Cingolani, A. M.: Livestock grazing affects microclimate conditions for decomposition process through changes in vegetation structure in mountain grasslands, Acta Oecologica, 91, 101–107, <https://doi.org/10.1016/j.actao.2018.07.002>, 2018.

Villarino, S. H., Pinto, P., Jackson, R. B., and Piñeiro, G.: Plant rhizodeposition: A key factor for soil organic matter formation 575 in stable fractions, Sci. Adv., 7, eabd3176, <https://doi.org/10.1126/sciadv.abd3176>, 2021.



Von Lützow, M., Kögel-Knabner, I., Ekschmitt, K., Flessa, H., Guggenberger, G., Matzner, E., and Marschner, B.: SOM fractionation methods: Relevance to functional pools and to stabilization mechanisms, *Soil Biol. Biochem.*, 39, 2183–2207, <https://doi.org/10.1016/j.soilbio.2007.03.007>, 2007.

Wei, Y., Xiong, X., Ryo, M., Badgery, W. B., Bi, Y., Yang, G., Zhang, Y., and Liu, N.: Repeated litter inputs promoted stable soil organic carbon formation by increasing fungal dominance and carbon use efficiency, *Biol. Fertil. Soils*, 58, 619–631, <https://doi.org/10.1007/s00374-022-01647-8>, 2022.

Wieder, W. R., Hartman, M. D., Sulman, B. N., Wang, Y., Koven, C. D., and Bonan, G. B.: Carbon cycle confidence and uncertainty: Exploring variation among soil biogeochemical models, *Glob. Change Biol.*, 24, 1563–1579, <https://doi.org/10.1111/gcb.13979>, 2018.

585 Wiesmeier, M., Urbanski, L., Hobley, E., Lang, B., Von Lützow, M., Marin-Spiotta, E., Van Wesemael, B., Rabot, E., Ließ, M., Garcia-Franco, N., Wollschläger, U., Vogel, H.-J., and Kögel-Knabner, I.: Soil organic carbon storage as a key function of soils - A review of drivers and indicators at various scales, *Geoderma*, 333, 149–162, <https://doi.org/10.1016/j.geoderma.2018.07.026>, 2019.

590 Witzgall, K., Vidal, A., Schubert, D. I., Höschen, C., Schweizer, S. A., Buegger, F., Pouteau, V., Chenu, C., and Mueller, C. W.: Particulate organic matter as a functional soil component for persistent soil organic carbon, *Nat. Commun.*, 12, 4115, <https://doi.org/10.1038/s41467-021-24192-8>, 2021.

Yang, Y., Gunina, A., Cheng, H., Liu, L., Wang, B., Dou, Y., Wang, Y., Liang, C., An, S., and Chang, S. X.: Unlocking Mechanisms for Soil Organic Matter Accumulation: Carbon Use Efficiency and Microbial Necromass as the Keys, *Glob. Change Biol.*, 31, e70033, <https://doi.org/10.1111/gcb.70033>, 2025.

595 Yin, Q., Liu, Y., Li, J., Wu, J., Wang, Y., Zhang, H., Liu, H., Jiang, L., Yang, J., Wang, Y., Jiang, Y., Han, X., and Wang, J.: Soil organic carbon formation in grassland ecosystems: Higher efficiency of roots than shoots and rhizodeposition, *Soil Tillage Res.*, 250, 106523, <https://doi.org/10.1016/j.still.2025.106523>, 2025.

Zhang, Y., Lavallee, J. M., Robertson, A. D., Even, R., Ogle, S. M., Paustian, K., and Cotrufo, M. F.: Simulating measurable ecosystem carbon and nitrogen dynamics with the mechanistically defined MEMS 2.0 model, *Biogeosciences*, 18, 3147–3171, <https://doi.org/10.5194/bg-18-3147-2021>, 2021.

600 Zhang, Y., King, A. E., Hamilton, E., and Cotrufo, M. F.: Representing cropping systems with the MEMS 2 ecosystem model, *Agron. J.*, 116, 2328–2345, <https://doi.org/10.1002/agj2.21611>, 2024.

Zhou, Z., Ren, C., Wang, C., Delgado-Baquerizo, M., Luo, Y., Luo, Z., Du, Z., Zhu, B., Yang, Y., Jiao, S., Zhao, F., Cai, A., Yang, G., and Wei, G.: Global turnover of soil mineral-associated and particulate organic carbon, *Nat. Commun.*, 15, 5329, <https://doi.org/10.1038/s41467-024-49743-7>, 2024.